Eur Biophys J (2003) 32: 381–391
DOI 10.1007/s00249-003-0281-3

ARTICLE

Mau Sinha · Sudha Mishra · Preeti G. Joshi

Liquid-ordered microdomains in lipid rafts and plasma membrane of U-87 MG cells: a time-resolved fluorescence study

Received: 11 July 2002 / Revised: 3 October 2002 / Accepted: 13 December 2002 / Published online: 6 March 2003

Abstract Lipid rafts, the functional microdomains in the cell membrane, are believed to exist as liquid-ordered (L_o) phase domains along with the liquid-disordered (L_d) phase of the bulk of the cell membranes. We have examined the lipid order in model and natural membranes by time-resolved fluorescence of trimethylammonium-1,6-diphenylhexatriene incorporated into the membranes. The lipid phases were discerned by the limiting anisotropy, rotational diffusion rate and distribution of the fluorescence lifetime. In dipalmitoylphosphatidylcholine (DPPC)-cholesterol mixtures the gel phase exhibited higher anisotropy and a two-fold slower rotational diffusion rate of the probe as compared to the L_d phase. On the other hand, the L_o phase exhibited higher limiting anisotropy but a rotational diffusion rate comparable to the L_d phase. The L_d and L_o phases elicited unimodal distribution of lifetimes with distinct mean values and their co-existence in phospholipid-cholesterol mixtures was reflected as a biphasic change in the width of the lifetime distribution. Global analysis of the lifetimes yielded a best fit with two lifetimes which were identical to those observed in single L_o or L_d phases, but their fractional contribution varied with cholesterol concentration. Attributing the shorter and longer lifetime components to the L_d and L_o phases, respectively, the extent of the L_o/L_d phase domains in the membranes was estimated by their fractional contribution to the fluorescence decay. In ternary mixtures of egg PC-gangliosides-cholesterol, the gangliosides induced heterogeneity in the membrane but the L_d phase prevailed. The L_o phase properties were observed only in the presence of cholesterol. Results obtained in the plasma membrane and detergent-resistant membrane fractions (DRMs) isolated from U-87 MG cells revealed that DRMs mainly possess the L_o phase; however, a substantially large proportion of plasma membrane also exists in the L_o phase. Our data show that, besides cholesterol, the membrane proteins play a significant role in the organization of lipid rafts and, furthermore, a considerable amount of heterogeneity is present among the lipid rafts.

Keywords Fluorescence · Lipid microdomains · Lipid rafts · Membranes · Trimethylammonium-1,6-diphenylhexatriene

Abbreviations DPPC: dipalmitoylphosphatidylcholine · DRM: detergent-resistant membrane fraction · EPC: egg phosphatidylcholine · GSL: glycosphingolipid · L_d: liquid-disordered phase domains · L_o: liquid-ordered phase domains · MBCD: methyl-β-cyclodextrin · PBS: phosphate buffered saline · PM: plasma membrane · TMA-DPH: trimethylammonium-1,6-diphenylhexatriene

Introduction

Several studies have suggested the existence of lipid microdomains in biological membranes. Recently, it was proposed that glycosphingolipids (GSLs) and high concentrations of cholesterol present in the plasma membrane could lead to the formation of lipid microdomains termed "lipid rafts" that attach specific membrane proteins (Rietveld and Simons 1998; Simons and Ikonen 1997). Lipid rafts have been implicated in important cellular functions such as intracellular sorting and signal transduction (Brown and Rose 1992; Kasahara and Sanai 1999; Kurzchalia and Parton 1999; Simons and Toomre 2000). The presence of lipid domains enriched in GPI-anchored proteins has been demonstrated in the plasma membrane of intact cells (Friedrichson and Kurzchalia 1998; Varma and Mayor 1998). Brown and co-workers proposed that lipid rafts might originate due to organization of certain lipids into

M. Sinha · S. Mishra · P.G. Joshi (✉)
Department of Biophysics,
National Institute of Mental Health and Neurosciences,
560 029 Bangalore, India
E-mail: pgjoshi@nimhans.kar.nic.in
Tel.: +91-80-6995102
Fax: +91-80-6564830

liquid-ordered (L_o) phase domains (Ahmed et al. 1997; Schroeder et al. 1994). The L_o phase is characterized by high order in the lipid acyl chains like the gel phase but with fast translational and rotational mobility like the L_d phase (Almeida et al. 1992; Vist and Davis 1990). Owing to the co-existence of these phases under certain conditions, phase separation may occur in the lipid bilayers, giving rise to lipid microdomains. The specific lipid moieties which would result in formation of the L_o phase are not yet clear. Both cholesterol and GSLs are good candidates; however, Ostermeyer et al. (1999) have suggested that GSLs are not essential for formation of the L_o phase.

The co-existence of liquid-disordered (L_d) and L_o phases in phospholipid-cholesterol bilayers has been demonstrated by EPR, NMR and fluorescence spectroscopic methods (Ipsen et al. 1987; Mateo et al. 1995; Sankaram and Thompson 1991). Using a fluorescence quenching method, Wang et al. (2000) have assessed the affinity of different phospholipids and some peptides to the L_o phase. Recently, the L_o/L_d phase domains in supported lipid monolayers and giant unilamellar vesicles have been visualized by confocal fluorescence microscopy (Dietrich et al. 2001; Korlach et al. 1999). However, the existence of L_o domains in cell membranes has not been conclusively demonstrated. It has mainly been inferred from the facts that the lipid mixtures which form L_o domains exhibit resistance to extraction by non-ionic detergents at low temperature (Schroeder et al. 1994) and a detergent-resistant low-density membrane fraction enriched in cholesterol, GSLs and specific signalling proteins can be isolated from the cell membranes (Brown and London 1997; Fra et al. 1994; Gorodinsky and Harris 1995; Rodgers et al. 1994). Ge et al. (1999) showed that the detergent-insoluble fractions isolated from RBL-2H3 mast cells exhibit higher order, a characteristic of the L_o phase. However, there has been a concern that detergent treatment could alter the composition and phase behavior of cell membranes (Brown and London 1998). In a recent report, Gidwani et al. (2001) showed that the plasma membrane of RBL-2H3 cells is substantially ordered.

In this study we have employed time-resolved fluorescence of a lipid-specific probe, trimethylammonium-1,6-diphenylhexatriene (TMA-DPH), to gauge the distribution of L_o and L_d phases in model and natural membranes. As the fluorescence characteristics of TMA-DPH are sensitive to its environment, it has been widely used to measure the order of lipid acyl chains in cell membranes and intact cells. In this paper we demonstrate the differential fluorescence lifetime, anisotropy and rotational diffusion of this probe in L_o and L_d phases of lipid bilayers and show that the relative extent of L_o/L_d phases in the membranes can be semi-quantitatively assessed by global analysis of the fluorescence lifetimes. The method was used to examine the L_o/L_d microdomains in the plasma membranes and detergent-insoluble membrane fractions isolated from U-87 MG cells.

Materials and methods

Materials

U-87 MG cells were obtained from the National Centre for Cell Sciences (Pune, India). Fetal calf serum was procured from GIBCO-BRL Life Technologies (New Delhi, India). TMA-DPH and Amplex red cholesterol assay kit were obtained from Molecular Probes (Eugene, Ore., USA) and all other chemicals were from Sigma (St. Louis, Mo., USA).

Preparation of liposomes

Unilamellar liposomes were prepared as described previously (Sanganahalli et al. 2000). Briefly, required quantities of lipids were dissolved in a chloroform-methanol mixture (1:1 v/v) and dried under a stream of nitrogen gas. Subsequently, a known volume of phosphate buffered saline (PBS) was added to the vials and kept at 37 °C for 10 min for the lipids to swell. The lipids were scraped from the surface of the vials into the buffer and the lipid suspensions were sonicated using a Vibra cell sonicator (Sonics and Materials, Danbury, Conn., USA) at a 40% duty cycle and power output of 20 W until the liposome suspensions became clear. The phospholipid concentration in the samples was 0.25 mg/mL. The bovine brain ganglioside mixture contained 19.8% GM1, 39.6% GD1a, 14.6% GD1b and 17.6% GT1b (Guerold et al. 1992). The concentration of individual gangliosides in the liposomes was calculated accordingly and their sum was taken as the total ganglioside concentration to estimate the phospholipid-ganglioside molar ratio. The molar concentration of egg phosphatidylcholine (EPC) was calculated by taking an average molecular weight of 760.08.

Cell culture and isolation of membranes

The cells were grown in EMEM supplemented with 1 mM sodium pyruvate, 5% fetal calf serum, 5% bovine serum, 2.2 g/L HEPES, 50,000 units/L benzylpenicillin, 3500 units/L streptomycin and 2.2 mg/L nystatin at 37 °C, as described by Joshi and Mishra (1992). Isolation of plasma membrane from cultured cells and assessment of membrane enrichment was performed as described earlier (Sreenivasan et al. 1997). To estimate membrane enrichment, a marker enzyme for the plasma membrane, Na^+-K^+-ATPase, was assayed. Different plasma membrane preparations were enriched 1.8- to 2.4-fold in Na^+-K^+-ATPase activity compared to the cell homogenate. This is consistent with enriched but not pure plasma membrane preparations. Detergent-resistant membrane fractions (DRMs) were isolated as described by Brown and Rose (1992), with some modifications. Confluent cells (250×10^6) were washed once with PBS, scraped with a rubber policeman in PBS and pelleted. The cells were treated with chilled lysis buffer (20 mM Tris-HCl, pH 6.5, 150 mM NaCl, 1 mM EDTA, 1% Triton X-100, 1 mM PMSF, 1 μg/mL each of aprotinin, leupeptin and pepstatin A) and kept in ice for 20 min. The lysate was homogenized with 30 strokes in a Dounce homogenizer and mixed with an equal volume of 80% sucrose in lysis buffer without detergent. Then 2 mL of this lysate were placed at the bottom of the centrifuge tube and layered on top with 6 mL of 22% and 2 mL of 5% sucrose in buffer, respectively. It was then centrifuged at 39,000 rpm for 12 h at 4 °C in a TH-641 swinging rotor (Sorvall Combiplus). The DRM was collected as the interface between the 22% and 5% sucrose gradients. The fraction was washed with PBS, pelleted and resuspended in the buffer.

Lipid extraction and estimation

Lipids were extracted from plasma membranes and DRMs according to Folch et al. (1957). The membranes were pelleted and treated with a cold chloroform-methanol mixture (2:1 v/v) and kept

in ice for 30 min. Samples were then centrifuged at 10,000 rpm for 5 min at 4 °C to separate the proteins and the clear chloroform-methanol layer containing total lipids was collected for preparation of liposomes and estimation of phospholipids, as described by Bartlett (1959), and cholesterol, as described by Amundson and Zhou (1999).

Depletion of cholesterol from the membranes

For depletion of cholesterol the membranes were incubated with methyl-β-cyclodextrin (MBCD) for 1 h at 37 °C (Gidwani et al. 2001). Control samples were incubated in buffer without MBCD under the same conditions. The membranes were collected by centrifugation and washed once with PBS. The extent of cholesterol depletion in given samples was quantified.

Labelling of liposomes and membrane vesicles with TMA-DPH

The liposomes and membrane vesicles were labelled with TMA-DPH as described previously (Ravichandra and Joshi 1999; Sharma et al. 1997). A working solution of TMA-DPH (4 μM) was prepared by slowly adding a specific volume of its stock solution in dimethylformamide to a known volume of vigorously stirred PBS. The dispersion was allowed to stir continuously for 1 h at 25 °C. For fluorescence measurements, a known volume of the working solution was added to a given volume of membranes. The final concentration of TMA-DPH in the sample was 2 μM. We also explored another method to incorporate the probe into the liposomes by adding the required volumes of TMA-DPH stock solution to lipid mixtures before drying. The samples were processed and sonicated as described above. Identical results were obtained with these two methods, so we subsequently followed the former procedure. Liposomes not labelled with the probe were used as blanks in the fluorescence measurements.

Measurement of steady-state fluorescence

The steady-state fluorescence intensity and anisotropy were measured with a SLM 8000C spectrofluorometer. The samples were excited at 337 nm to measure the fluorescence spectra. For anisotropy measurements, Glan Thompson prism polarizers were used in the optical paths. Samples were excited at 337 nm with vertically polarized light and vertical (I_{vv}) and horizontal (I_{vh}) polarized fluorescence intensities were measured simultaneously using a T-geometry optical path. The anisotropy (r) was calculated as:

$$r = I_{vv} - I_{vh}/I_{vv} + 2GI_{vh} \quad (1)$$

where G is the correction factor given by $G = I_{hv}/I_{hh}$. Anisotropy values were calculated after subtracting appropriate blanks.

Time-resolved fluorescence measurements and data analysis

The time-resolved fluorescence intensity and anisotropy were measured with a FLA900 spectrofluorometer (Edinburgh Instruments) using the single-photon counting mode. Each sample decay curve data were acquired to give a peak count of 5000 and a corresponding lamp profile was collected using a scattering solution. To measure the decay of fluorescence anisotropy, Glan Thompson polarizers were placed in the excitation and emission path. Decays of vertically, $I(t)_{vv}$, and horizontally, $I(t)_{vh}$, polarized fluorescence intensities were measured by toggling the emission polarizer between vertical and horizontal positions and simultaneously acquiring the data in two memory segments of a multichannel analyzer (MCA).

The fluorescence intensity decays were analyzed by multiexponential and distribution analysis using the FLA-900 software (Edinburgh Instruments). The fluorescence intensity decay is represented by a sum of individual exponentials:

$$I(t) = \sum \alpha_i \exp(-t/\tau_i) \quad (2)$$

where τ_i are the individual decay times and α_i the associated pre-exponential factors. The fractional contribution of the ith component to the total intensity is given by:

$$f_i = \alpha_i \tau_i / \sum \alpha_i \tau_i \quad (3)$$

The distribution model fits the data to a discrete set of exponentials evenly spaced in lifetime, with amplitudes determined by a continuous distribution. The relative weighting of each lifetime is calculated as:

$$f_j = \sum_i (B_{ji} \Delta\tau_{ji} \tau_{ji}) / \sum_j \sum_i (B_{ji} \Delta\tau_{ji} \tau_{ji}) \quad (4)$$

where i is each amplitude within a peak and j is each peak within the complete fit. The decay parameters are recovered using the nonlinear least-square iterative fitting procedure based on the Marquardt algorithm by varying the center lifetime (τ_c) and the width of the distribution (F_w). The goodness of fit was judged by the reduced χ^2 parameter and the weighted residuals.

The decay of fluorescence anisotropy was analyzed according to the wobbling in cone model. The fluorophore in the membrane is considered to be in a hindered environment and the decay of fluorescence anisotropy is represented by:

$$r(t) = (r_0 - r_\infty)\exp(-t/\phi) + r_\infty \quad (5)$$

where r_0 is the anisotropy at $t = 0$, r_∞ is the limiting anisotropy and ϕ is the rotational correlation time. The rotational rate (R) of the fluorophore was calculated based on the equation:

$$1/\phi = 6R \quad (6)$$

Global analysis of fluorescence lifetimes

The above analysis is useful to obtain an accurate and unbiased representation of individual decay curves. However, the global analysis model allows simultaneous analysis of a family of decay curves in terms of internally consistent sets of fitting parameters. Such analysis is useful for determining the intrinsic relationship that may exist between the decay curves obtained under variable conditions and is extremely useful in evaluating the manner in which the decay parameters vary as a function of an independent variable (Beecham et al. 1991; Rawat et al. 1997).

We obtained the fluorescence decays with varying lipid composition. The global analysis was done by linking the lifetimes among data files so that they are held in common between the decay curves, but the pre-exponentials were allowed to vary. The data files were simultaneously analyzed by a least-square fitting procedure using the Marquardt algorithm. The fit was judged by the weighted residuals and the global χ^2 parameter, which was generally less than 1.7.

Determination of the partition coefficient of TMA-DPH in different membranes

The partitioning of TMA-DPH in membranes of different composition used in this study was measured as described by Huang and Haugland (1991). The fluorescence intensity of TMA-DPH in liposomes was measured with an increasing lipid/probe ratio, keeping the probe concentration constant at 2 μM. The total lipid concentration was varied from 10 μM to 400 μM. In liposomes constituted of mixed lipids, the ratio of mole concentration of lipids was held constant. The fluorescence intensity (F) increases with increasing lipid concentration (L) and finally saturates at F_0. The partition coefficient (K_p) between lipid and water was estimated from the x-intercept of the double reciprocal plot given by the following equation:

$$1/F = [55.6/(K_p F_0)](1/L) + 1/F_0 \quad (7)$$

Results

The existence of two fluid phases in dipalmitoylphosphatidylcholine (DPPC)-cholesterol binary mixtures is well established (Sankaram and Thompson 1991; Vist and Davis 1990). We used this lipid system to assess the ability of TMA-DPH to distinguish between the two fluid phases in the lipid bilayers. The fluorescence properties of this probe in liposomes made up of DPPC-cholesterol mixtures representing different lipid phases were examined under appropriate experimental conditions.

Fluorescence anisotropy of TMA-DPH in DPPC-cholesterol mixtures

In DPPC bilayers the transition from the gel to the L_d phase occurs at about 41.5 °C; therefore we chose pure DPPC liposomes at 25 °C and 50 °C as representatives of the gel and L_d phases, respectively. Cholesterol induces formation of the L_o phase in DPPC bilayers and the phase diagram for DPPC-cholesterol mixtures as determined by NMR and EPR spectroscopy shows that, above the phase transition temperature, lipid bilayers constituted by DPPC and 30 mol% cholesterol exist in the L_o phase (Sankaram and Thompson 1991; Vist and Davis 1990). The fluorescence anisotropy of DPH and its derivatives has been extensively used to study the phase transition in membranes (Bernsdorff et al. 1997; Lentz et al. 1976, 1980; Shinitzky and Barenholz 1978). We found that the steady-state anisotropy of TMA-DPH in DPPC at 25 °C (gel phase) was 0.321 ± 0.010 and it decreased to 0.183 ± 0.001 at 50 °C (L_d phase); in the presence of 30 mol% cholesterol (L_o phase), an intermediate value of 0.237 ± 0.007 was observed. These results are suggestive of the ordering of lipid acyl chains in the gel and L_o phases. However, no clear distinction could be made between the two phases. Since the L_o phase is characterized by highly ordered lipid acyl chains and high rotational and lateral mobility, we further determined the rotational mobility of the probe in these samples by measuring the time-resolved anisotropy. As shown in Fig. 1, the decay of the fluorescence anisotropy in the gel phase (curve a) was considerably slower than that observed in the fluid phases (curves b and c). Analysis of the decay curves (Table 1) showed that the rotational diffusion rate of TMA-DPH was comparable in the L_d and L_o phases, but it was more than two-fold slower in the gel phase. The limiting anisotropy was higher in the gel and L_o phases as compared to the L_d phase. Thus, the typical characteristics of gel, L_d and L_o phases are clearly affirmed by the time-resolved fluorescence anisotropy measurements.

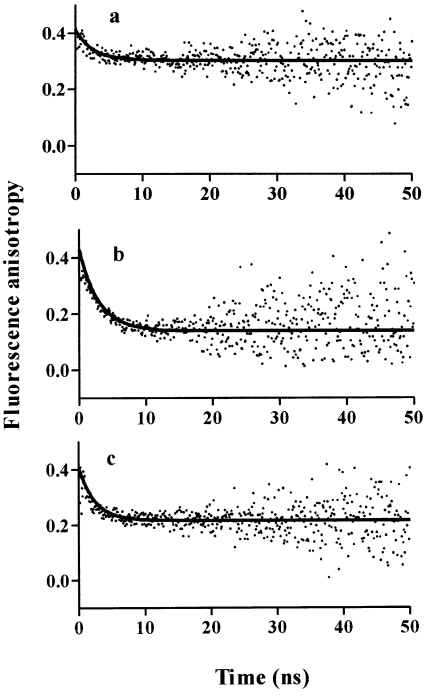

Fig. 1 Decay of fluorescence anisotropy of TMA-DPH in DPPC liposomes at (**a**) 25 °C, (**b**) 50 °C and (**c**) DPPC with 30 mol% cholesterol at 50 °C. *Dots* represent the experimental data and *solid lines* represent the fitted curves

Table 1 Rotational rate (R) and limiting anisotropy (r_∞) of TMA-DPH in DPPC-cholesterol liposomes[a]

Sample	R (10^8/s)	r_∞
DPPC (25 °C)	0.302 ± 0.028	0.32 ± 0.01
DPPC (50 °C)	0.609 ± 0.020	0.14 ± 0.01
DPPC + 30 mol% chol. (50 °C)	0.704 ± 0.017	0.21 ± 0.00

[a]The lipid composition and temperatures shown here were selected to represent gel (DPPC at 25 °C), liquid disordered (DPPC at 50 °C) and liquid ordered (DPPC-30 mol% cholesterol at 50 °C) phases. The data are the mean ± SD of three experiments

Fluorescence lifetime of TMA-DPH

The fluorescence lifetime is a good indicator of the microenvironment of the fluorescence probe. Earlier studies have shown that DPH and TMA-DPH exhibit differential lifetimes in the gel and L_d phases (Barrow and Lentz 1985; Prendergast et al. 1981). We analyzed the decay of the fluorescence intensity for 100 lifetimes between 0.05 and 100 ns. As shown in Table 2, the distribution of lifetimes was markedly different in three lipid phases. DPPC at 25 °C (gel phase) exhibited a bimodal distribution of lifetimes centered at 1.99 ± 0.25 ns and 6.66 ± 0.09 ns with a fractional contribution of 0.09 and 0.91, respectively. At 50 °C the distribution was unimodal, with the lifetime centers located at 3.51 ± 0.23 ns and 6.84 ± 0.41 ns in the absence (L_d) and presence of 30 mol% cholesterol (L_o), respectively. Also an appreciable increase was observed in F_w (full width at half maximal of distribution) in the L_o phase and it

Table 2 Distribution analysis of fluorescence life times of TMA-DPH in DPPC-cholesterol liposomes[a]

Sample	τ_1 (ns)	F_{w1} (ns)	τ_2 (ns)	F_{w2} (ns)
DPPC (25 °C)	1.99 ± 0.25 (0.09 ± 0.03)	0.42 ± 0.00	6.66 ± 0.09 (0.91 ± 0.03)	1.37 ± 0.19
DPPC (50 °C)	3.51 ± 0.23 (1.00 ± 0.00)	0.53 ± 0.12	–	–
DPPC + 30 mol% chol. (50 °C)	–	–	6.84 ± 0.41 (1.00 ± 0.00)	1.00 ± 0.04

[a]The distribution was bimodal in the gel phase (DPPC at 25 °C) but unimodal in the liquid disordered (DPPC at 50 °C) and liquid ordered (DPPC-30 mol% cholesterol at 50 °C) phases. τ and F_w represent the mean value and half-width of the lifetime distribution, respectively. The numbers in parentheses show the fractional contribution. The data are the mean ± SD of three experiments

further increased in the gel phase (Table 2). These data reveal that TMA-DPH exhibits differential lifetimes not only in the gel and L_d phases but also in the L_o phase. The bimodal and broader distribution in the gel phase indicates greater heterogeneity, possibly due to the immobility of lipids. In some samples a short lifetime component of 0.45 ± 0.20 ns was observed; however, its fractional contribution was less than 0.001, hence it was ignored. This component is believed to occur due to the oxidation of TMA-DPH (Straume and Litman 1987; Williams and Stubbs 1988).

Fluorescence characteristics of TMA-DPH in mixed L_d/L_o phases

It is widely accepted that biological membranes lack the gel phase and the L_o phase is considered as the main feature of the lipid rafts in the membrane. Our subsequent experiments were focused on mixed L_d/L_o phases. DPPC liposomes were prepared with varying concentrations of cholesterol and experiments were performed at 50 °C to ensure the fluid phase. As depicted in Fig. 2, the fluorescence intensity and steady-state anisotropy of TMA-DPH was enhanced by cholesterol in a concentration-dependent manner (panels a and b). This effect could be attributed to the increased packing of lipid bilayers by cholesterol, which makes the membranes more ordered and reduces the water permeability (Bernsdorff et al. 1997). The fluorescence lifetime distributions were unimodal at all cholesterol concentrations, but the center of the distribution shifted to higher values with increasing cholesterol concentrations (panel c). Interestingly, upon increasing the cholesterol content, the half-width of the lifetime distribution F_w was also enhanced up to 20 mol%, suggesting increased heterogeneity in the samples which then diminished at higher cholesterol concentrations (panel d). These data indicate the existence of mixed phases in the liposomes.

In view of the fact that TMA-DPH exhibited distinct lifetimes in the L_d and L_o phases, we performed a global analysis of the decay curves obtained at different cholesterol concentrations. Discrete lifetimes were linked between all the decay curves and the pre-exponential factors were allowed to vary. The least-square analysis yielded the best fit with two lifetimes of 3.50 ± 0.13 ns and 7.02 ± 0.32 ns and the global $\chi^2 = 1.53$. The contribution of the two lifetime components varied with cholesterol concentration. As shown in Fig. 3, at 0 mol% cholesterol the fractional contribution of the shorter lifetime was 0.983 ± 0.024. With increasing cholesterol concentration the contribution of the longer lifetime component continuously increased at the expense of the shorter lifetime component and at 50 mol% cholesterol it was 0.983 ± 0.022. We infer that the two lifetime components described here arise due to the localization of TMA-DPH in the L_d and L_o phase domains and their fractional contributions indicate the relative extent of these two fluid phases in the membranes.

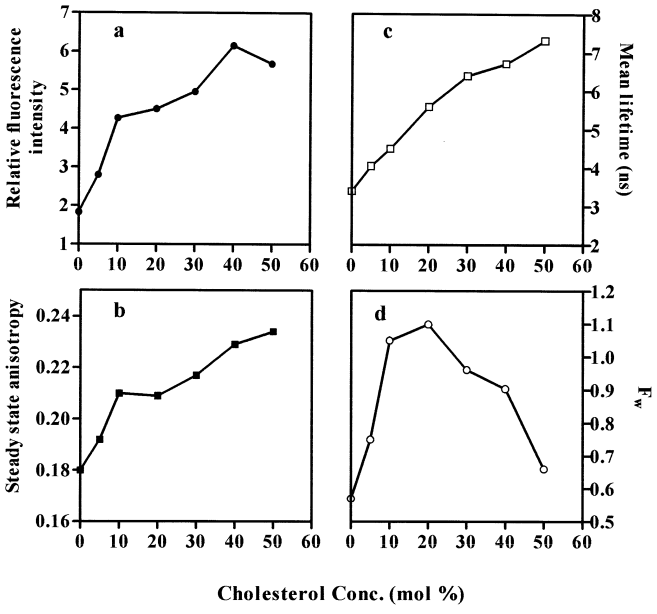

Fig. 2a–d Effect of cholesterol concentration on the fluorescence characteristics of TMA-DPH in DPPC liposomes at 50 °C. Changes in (**a**) fluorescence intensity, (**b**) steady-state anisotropy, (**c**) fluorescence lifetime and (**d**) half-width of lifetime distribution are shown as a function of cholesterol concentration

Fluorescence characteristics of TMA-DPH in phospholipid-ganglioside-cholesterol ternary mixtures

GSLs and cholesterol are enriched in the plasma membrane and are considered to play an important role in the formation of the L_o phase domains in the natural membranes (Harder and Simons 1997; Simons and Ikonen 1997). Unlike DPPC, which has saturated fatty acyl chains, most of the biological membranes contain unsaturated fatty acyl chains and their melting temper-

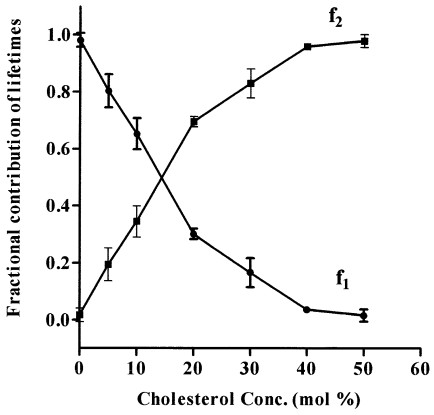

Fig. 3 Change in the fractional contribution of two fluorescence lifetimes of TMA-DPH in DPPC liposomes with varying cholesterol concentration. Fractional contribution of the shorter lifetime $\tau_1 = 3.50$ ns is represented by f_1 (*circles*) and that of the longer lifetime $\tau_2 = 7.02$ ns by f_2 (*squares*). The measurements were performed at 50 °C. The data are the mean ± SD of three experiments

atures are below 0 °C. EPC contains a mixture of phospholipids with large amounts of unsaturated fatty acyl chains. Thus a EPC-ganglioside-cholesterol mixture is a better representative of the natural membranes. The results obtained in EPC-cholesterol liposomes (in the absence of GSL) were quite similar to those observed in DPPC-cholesterol liposomes. The fluorescence intensity and steady-state anisotropy increased in cholesterol-containing samples (data not shown). Figure 4 shows the center and half-width of the lifetime distribution in liposomes comprising EPC-ganglioside-cholesterol mixtures. The lifetime distributions were unimodal in all cases. The presence of cholesterol increased the lifetime of TMA-DPH in EPC liposomes (panel a) and also increased the distribution width (panel b). Unlike DPPC-cholesterol mixtures, the biphasic change in F_w was not observed, possibly due to the compositional complexity of the EPC. The presence of 5 mol% gangliosides slightly increased the lifetime values; however, a marked increase was seen in F_w, suggesting that gangliosides enhance the heterogeneity in the bilayers. Increasing the ganglioside concentration to 10 mol% did not cause any further change in the lifetime or F_w. Global analysis of the fluorescence decay curves again showed the best fit with two lifetimes of $\tau_1 = 3.25 \pm 0.21$ ns and $\tau_2 = 6.54 \pm 0.26$ ns with a global χ^2 value of 1.44. In EPC-cholesterol liposomes the fractional contribution of the longer lifetime (f_2) increased from 0.08 at 0 mol% cholesterol to 0.94 at 50 mol%. These data show that cholesterol creates L_o domains in EPC bilayers also. The change in f_2 observed in EPC-ganglioside-cholesterol liposomes of varied composition is depicted in Fig. 5. In the absence of cholesterol, gangliosides (10 mol%) slightly increased f_2. In the presence of 5–20 mol% cholesterol, gangliosides did not cause any significant change; however, at higher cholesterol concentrations a small but significant reduction in f_2 was observed. We further examined the effect of gangliosides by

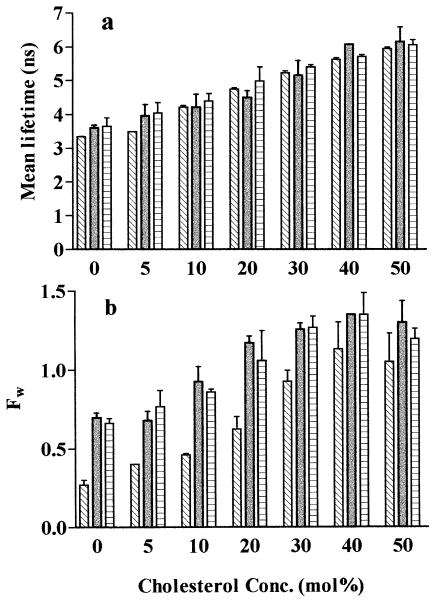

Fig. 4 The fluorescence lifetime (**a**) and half-width of lifetime distribution F_w (**b**) of TMA-DPH in EPC-ganglioside-cholesterol mixtures at 25 °C. Liposomes were prepared with DPPC in the absence (*slanted lines*) or presence of approximately 5 mol% (*filled bars*) and 10 mol% (*horizontal lines*) of mixed gangliosides and varying concentrations of cholesterol. The data are the mean ± SD of three experiments

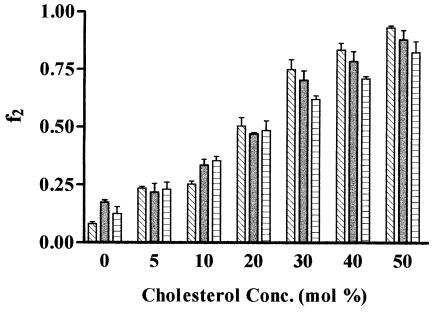

Fig. 5 Changes in the fractional contribution f_2 of the longer fluorescence lifetime component ($\tau_2 = 6.54$ ns) in EPC liposomes containing 0 mol% (*slanted lines*), 5 mol% (*filled bars*) and 10 mol % (*horizontal lines*) gangliosides at varying concentrations of cholesterol. The fractional contribution of the shorter lifetime component f_1 changed in a complimentary manner but only f_2 is shown for clarity. Measurements were performed at 25 °C. The data are the mean ± SD of three experiments

time-resolved fluorescence anisotropy measurements and the data are given in Table 3. The limiting anisotropy was slightly higher in EPC liposomes containing 5 mol% and 10 mol% gangliosides. In liposomes containing 30 mol% cholesterol, the limiting anisotropy was markedly higher and gangliosides did not bring about any appreciable change. The rotational diffusion rate was unaffected by the presence of cholesterol or gangliosides. These results clearly demonstrate the induction of L_o domains by cholesterol and gangliosides do not appear to facilitate this process.

Fluorescence characteristics of TMA-DPH in natural membranes

After establishing the method to identify the L_o/L_d microdomains in liposomes, it was further used in the detergent-insoluble membrane fraction (DRM) and enriched plasma membrane (PM) isolated from U-87 MG cells. As given in Table 4, the DRM exhibited a high limiting anisotropy (0.240 ± 0.008) and rotational rate (0.607×10^8/s), indicative of the L_o phase. The limiting anisotropy in the plasma membrane (0.225 ± 0.005) was considerably higher than that observed in the L_d phase in liposomes, suggesting that a considerable amount of order exists in the plasma membranes. Depletion of cholesterol from the membranes by MBCD treatment caused a decrease in the fluorescence anisotropy without a significant change in the rotational rate, indicating decreased order in the membranes. Under the given experimental conditions, the cholesterol concentration was decreased by 45% and 52% in the DRM and PM, respectively.

Table 3 Rotational rate (R) and limiting anisotropy (r_∞) of TMA-DPH in EPC-ganglioside-cholesterol liposomes[a]

Sample	R (10^8/s)	r_∞
EPC	0.428 ± 0.037	0.15 ± 0.01
EPC + 30 mol% chol.	0.480 ± 0.000	0.21 ± 0.01
EPC + 5 mol% GSL	0.468 ± 0.022	0.16 ± 0.00
EPC + 5 mol% GSL + 30 mol %chol.	0.453 ± 0.042	0.21 ± 0.00
EPC + 10 mol% GSL	0.445 ± 0.070	0.16 ± 0.00
EPC + 10 mol% GSL + 30 mol %chol.	0.428 ± 0.065	0.22 ± 0.01

[a]The data are the mean ± SD of three experiments

Table 4 Time-resolved analysis of limiting anisotropy (r_∞) and rotational rate (R) of TMA-DPH in membranes[a]

Sample	R (10^8/s)	r_∞
DRM	0.607 ± 0.080	0.240 ± 0.008
DRM, MBCD treated	0.520 ± 0.067	0.201 ± 0.011
DRM, lipid extract	0.534 ± 0.034	0.240 ± 0.010
PM[b]	0.537 ± 0.047	0.225 ± 0.005
PM, MBCD treated[b]	0.449 ± 0.035	0.180 ± 0.010
PM, lipid extract[b]	0.525 ± 0.046	0.205 ± 0.005

[a]The data represent the mean ± SD of three experiments
[b]PM denotes enriched plasma membrane preparation and not pure plasma membranes as mentioned in the Materials and methods section

The results of the distribution analysis of the fluorescence lifetimes in the DRM and PM are given in Table 5. The DRM exhibited a unimodal distribution of lifetimes with a mean value of 6.54 ± 0.32 ns ($\chi^2 = 1.489$), whereas the plasma membrane showed a bimodal distribution with mean lifetimes of 1.56 ± 0.08 ns and 5.66 ± 0.11 ns ($\chi^2 = 1.357$). The half-width of the longer lifetime components in the DRM (1.42 ns) and PM (1.56 ns) was quite large as compared to pure L_o (1.0 ns) or L_d (0.53 ns) phases in model membranes, indicating greater heterogeneity in the natural membranes. Depletion of cholesterol drastically decreased F_w and shifted the mean lifetime towards slightly lower values both in the DRM and PM, suggesting disordering of the membranes. The origin of the shorter lifetime component in the plasma membrane is not known at present.

In liposomes prepared with lipid extracts from the DRM, the limiting anisotropy was comparable to that observed in the DRM, whereas the fluorescence lifetime was decreased to 5.88 ± 0.04 and F_w decreased to 0.76 ± 0.11 ($\chi^2 = 1.291$). In the case of liposomes prepared from PM lipid extract, a significant decrease was observed in the limiting anisotropy (0.205 ± 0.005), lifetime and F_w; however, the distribution remained bimodal with mean lifetimes of 1.11 ± 0.25 ns and 4.05 ± 0.01 ns ($\chi^2 = 1.34$). These results are contrary to the effects expected due to the dynamic quenching of TMA-DPH by membrane proteins and thus imply that proteins also contribute to the ordering of microdomains in the membranes.

To estimate the L_o/L_d phases in these membranes, a global analysis of the fluorescence decay curves was performed by linking the lifetimes. The analysis yielded the best fit with two lifetimes of 2.395 ± 0.13 ns and 5.92 ± 0.28 ns and the global χ^2 value was 1.673. As shown in the last column of Table 5, the percentage of τ_2, which is indicative of the extent of L_o domains in the membrane, was $89 \pm 2\%$ in the DRM and $71 \pm 4\%$ in the PM. MBCD treatment decreased it to $63 \pm 3\%$ and $40 \pm 5\%$ in the DRM and PM, respectively. Membranes prepared with lipid extracts from the DRM and PM showed a $74 \pm 2\%$ and $41 \pm 1\%$ contribution of τ_2, respectively.

Table 5 Distribution analysis of fluorescence lifetimes of TMA-DPH in membranes[a]

Sample	τ_1 (ns)	F_{w1} (ns)	τ_2 (ns)	F_{w2} (ns)	f_2 (global analysis)
DRM	–	–	6.54 ± 0.32 (1 ± 0.0)	1.42 ± 0.21	0.89 ± 0.02
DRM, MBCD treated	–	–	5.56 ± 0.11 (1 ± 0.0)	0.75 ± 0.16	0.63 ± 0.03
DRM, lipid extract	–	–	5.88 ± 0.04 (1 ± 0.0)	0.76 ± 0.11	0.74 ± 0.02
PM[b]	1.56 ± 0.08 (0.07 ± 0.01)	0.38 ± 0.06	5.66 ± 0.11 (0.93 ± 0.01)	1.56 ± 0.08	0.71 ± 0.04
PM, MBCD treated[b]	1.66 ± 0.24 (0.15 ± 0.02)	0.40 ± 0.05	4.07 ± 0.03 (0.85 ± 0.2)	0.71 ± 0.07	0.40 ± 0.05
PM, lipid extract[b]	1.11 ± 0.25 (0.17 ± 0.03)	0.09 ± 0.01	4.05 ± 0.01 (0.83 ± 0.03)	0.78 ± 0.23	0.41 ± 0.01

[a]Numbers in parentheses show the fractional contribution. The last column shows the fractional contribution (f_2) of the longer lifetime component (5.92 ± 0.28 ns) obtained by global analysis of the fluorescence decays.The data are the mean ± SD of three experiments
[b]PM denotes enriched plasma membrane preparation and not pure plasma membranes as mentioned in the Materials and methods section

Discussion

The results presented in this paper demonstrate the sensitivity of the fluorescence characteristics of TMA-DPH to different lipid phases. Partitioning of amphiphilic probes in different lipid membranes can vary, which in turn may influence their fluorescence characteristics. Therefore it is important to consider the partitioning behavior of TMA-DPH in different membranes used in the present study. As given in Table 6, the partition coefficient of TMA-DPH was comparable in liposomes representing L_o and L_d phases. The ratio of partition coefficients in the L_o to L_d phases was 1.06 and 1.14 in the case of DPPC and EPC, respectively, suggesting that TMA-DPH would be distributed equally in coexisting L_o/L_d phases. Also the presence of gangliosides did not alter the partition coefficient appreciably. Similar partitioning behavior has been reported for DPH-PC by Gidwani et al. (2001). Thus the changes in the fluorescence properties of TMA-DPH described here are true reflections of the characteristics of the lipid phases.

The initial experiments were performed with well-characterized DPPC-cholesterol binary mixtures. Pure DPPC liposomes exhibited markedly higher fluorescence intensity, lifetime and steady-state anisotropy of TMA-DPH in gel phase (at 25 °C) as compared to the L_d phase (at 50 °C). Inclusion of cholesterol into the liposomes also increased the intensity, lifetime and steady-state anisotropy, indicating the ordering of the lipid bilayer by cholesterol. Lowering the temperature or increasing the cholesterol concentration had a similar effect on these fluorescence parameters; thus no distinction could be made between the gel phase and the L_o phase expected to be present under the respective conditions. Nonetheless, the time-resolved fluorescence anisotropy data revealed that the rotational diffusion rate of the probe in the gel phase (DPPC at 25 °C) was two-fold slower as compared to that in the L_d phase (DPPC at 50 °C). In the L_o phase (DPPC + 30 mol% cholesterol at 50 °C) the rotational diffusion rate was as high as in the L_d phase (Table 1). The limiting anisotropy value, an indicator of the order in the lipid acyl chains, was 0.32 and 0.14 in the gel and L_d phases, whereas an intermediate value of 0.21 was observed in the L_o phase. These data conform to the characteristics of the L_o phase in DPPC-cholesterol mixtures. The lifetimes of TMA-DPH in the L_d phase liposomes were distributed around the peak at about 3.51 ns with a half-width of 0.53 ns. In the L_o phase the center of lifetime distribution increased to 6.84 ns with a half-width of 1.0 ns. The ordering of lipid bilayers in the L_o and gel phases restricts water permeation into the membrane and thus enhances the fluorescence intensity and lifetime of the probe (Bernsdorff et al. 1997). We further examined the mixed L_o/L_d phases by varying the cholesterol concentration in DPPC liposomes. Careful analysis of fluorescence decay curves in different samples revealed interesting results. The fluorescence lifetime continuously increased upon increasing the cholesterol concentrations from 5 to 50 mol%. Notably, the half-width of the distribution changed in a biphasic manner (Fig. 2, panel d). The width of the lifetime distribution indicates the heterogeneity in the microenvironment of the probe. Such heterogeneity arises due to compositional and organizational factors or the solvent effect (Williams and Stubbs 1988). We infer that under the given experimental conditions the biphasic change in the distribution width arises due to the co-existence of L_d/L_o phases in the liposomes. The heterogeneity was a maximum at 20 mol% cholesterol and it diminished at higher or lower concentrations, indicating the predominance of one phase over the other. Narrowing of the distribution at 30 mol% and above indicates the predominance of the L_o phase. These data are consistent with the previously described phase behavior of DPPC-cholesterol (Sankaram and Thomson 1991; Huang et al. 1993; Xiang and Anderson 1998). Since the fluorescence lifetimes of TMA-DPH were unambiguously distinct in the L_o and L_d phases (Table 2), we explored the possibility of assessing the extent of two fluid phases in the liposomes by global analysis of the decay curves obtained with different cholesterol concentrations. The experiments were done at 50 °C to ensure the fluid phases in the liposomes. Global analysis of the decay curves by linking the lifetimes yielded best fits with two lifetimes of 3.50 ± 0.13 ns and 7.02 ± 0.32 ns. Within experimental error limits, these values were almost the same as those obtained by distribution analysis. These lifetimes can be attributed to the L_d and L_o phases, respectively, as they were approximately the same as the centers of lifetime distributions obtained by individual analysis of the decay curves obtained without and with 50 mol% cholesterol. The fractional contributions of the two lifetime components in liposomes containing different concentrations of cholesterol were in conformity to our contention. In the absence of cholesterol the contribution of τ_1 was 98.3% and with increasing cholesterol concentration the fractional contribution of τ_2 increased, finally reaching 98.4% at 50 mol% cholesterol. Thus it is evident that the relative extent of the two fluid phases in the membranes can be semi-quantitatively estimated by the global analysis method. It should be noted that the presence of two lipid phases was established by other parameters, such as rotational diffusion rate and half-width of the lifetime distributions.

The study was extended to liposomes constituted with ternary mixtures of EPC-gangliosides-cholesterol, a

Table 6 Partition coefficient (K_p) of TMA-DPH in different lipid membranes

Sample	K_p
DPPC	9.45×10^5
DPPC + 30 mol% chol.	8.90×10^5
EPC	8.90×10^5
EPC + 30 mol% chol.	7.78×10^5
EPC + 10 mol% GSL	7.78×10^5

system that mimics the lipid composition of the plasma membrane. Like the natural membranes, EPC contains a mixture of phospholipids with a large amount of unsaturated fatty acyl chains and gangliosides, the major glycosphingolipids of the neuronal cell membranes, can constitute up to 10% of the total lipids (Derry and Wolfe 1967). The mole fractions of gangliosides and cholesterol used in our experiments are in the physiological range. The fluorescence anisotropy and lifetime of TMA-DPH show that EPC liposomes at room temperature exist in the L_d phase. Incorporation of cholesterol increased the fluorescence intensity, anisotropy and lifetime of the probe, reflecting the ordering of fatty acyl chains by cholesterol. Global analysis of fluorescence lifetimes also showed the increase in the L_o domains, as reflected in the fractional contribution of the two lifetimes. Earlier studies have reported the existence of ordered microdomains in unsaturated PC-cholesterol mixtures (Mateo et al. 1995; Mitchell and Litman 1998; Straume and Litman 1987). Gangliosides caused a very small rise in the mean lifetime value and a modest increase in the fluorescence anisotropy. These results are consistent with earlier studies, which showed that, at low mole fractions ($<24\%$), gangliosides are randomly mixed in phospholipid bilayers and do not form micellar structures (Bunow and Bunow 1979; Sillerud et al. 1979; Hinz et al. 1981). Global analysis of the lifetimes did not elicit any appreciable shift in the fractional contributions of the two lifetimes in liposomes containing gangliosides, implying that the lipid bilayer maintains the L_d phase. The orderliness was inducted by cholesterol, which was manifested as the drastic increase in the anisotropy and fractional contribution of the longer lifetime component. Notably, a 2.5-fold increase was observed in F_w in the presence of 5 mol% and 10 mol% gangliosides. Such extensive broadening of the lifetime distribution is suggestive of a greatly heterogeneous microenvironment for the fluorescence probe.

Several spectroscopic methods have been employed previously to characterize the L_o phase domains in model membranes. These methods invariably involve incorporation of labelled phospholipids in the bilayer that limits their applicability in the natural membranes. Our study has put forward a novel method for semiquantitative detection of fluid phase microdomains in the membranes. We have used this method to examine the fluid phase domains in the cell membranes and detergent-resistant membrane fractions isolated from U-87 MG cells. The high fluorescence anisotropy and rotational rate of TMA-DPH in DRMs were characteristic of the L_o phase. The role of cholesterol and proteins in the organization of phase domains was examined by depletion of cholesterol or by extraction of lipids from the membranes. The anisotropy and lifetime values decreased appreciably in cholesterol-depleted DRMs, whereas removal of proteins did not have a significant effect. These results confirm that cholesterol is the major player in the packing of L_o domains in DRMs. Plasma membranes showed anisotropy values lower than DRMs, but it was considerably higher than the values obtained in the L_d phase in DPPC or EPC liposomes. Depletion of cholesterol from PMs decreased the anisotropy. Removal of proteins also caused a reduction in the anisotropy value. The differences in the membrane order elicited as the changes in the limiting anisotropy were also reflected in the fluorescence lifetime. The lifetime of the probe in more ordered membranes was enhanced. Analysis of fluorescence decays showed a very wide distribution of lifetimes in the PMs, eliciting the heterogeneity in the membrane. Interestingly, even the DRMs, exhibiting the characteristics of L_o phase, showed a large heterogeneity. Global analysis of fluorescence decay curves was performed to estimate the contribution of the L_o/L_d phases in natural membranes. As shown in the last column of Table 5, the extent of the L_o domains in the membrane varied greatly between different samples. Our analysis showed that the DRMs exist largely as the L_o phase (89% L_o); nevertheless, 71% of the PMs also exist in the ordered phase. We would like to mention here that the purity of the PM may have some bearing on the results. In case of contamination with other intracellular membranes, which would most likely be in the L_d phase, the measured values in the PM would be an underestimation of the L_o phase. We cannot completely rule out the residual presence of intracellular membranes in our PM preparations; however, as described in the Materials and methods section, the membrane preparations were reasonably enriched in marker enzyme activity and the contamination is expected to be minimal. Depletion of cholesterol drastically diminished the L_o domains in both in the PM and DRM. Quantitative measurement of phospholipids and cholesterol in our samples revealed that the PM and DRM contained 27.91 ± 0.12 and $47.90 \pm 2.20\%$ cholesterol, respectively. After MBCD treatment it reduced to $13.39 \pm 0.06\%$ in the PM and $26.34 \pm 1.20\%$ in DRM, which is incidentally comparable to that obtained in the untreated PM. However, the limiting anisotropy and the fraction of the long lifetime component was considerably lower in MBCD-treated DRMs as compared to PMs (Tables 4 and 5). There are gross differences in lipid and protein composition of these two membranes; even so, the lipids sorted into DRMs are expected to favor the L_o phase. On the contrary, the order was relatively higher in PMs as compared to DRMs containing comparable amounts of cholesterol (after MBCD treatment). These observations lead us to infer that besides cholesterol, membrane proteins could also be involved in ordering the L_o microdomains. Furthermore, the L_o phase drastically diminished in liposomes prepared with lipid extracts of PMs and DRMs. Since the lipid bilayers prepared from lipid extracts are expected to be bilaterally symmetric and thus different from the bilaterally asymmetric PM bilayer, a quantitative comparison was not attempted in this case. Nevertheless, these results support our notion that a considerable amount of order is brought about by membrane proteins.

Glycosphingolipids and cholesterol are considered as the basic molecular units responsible for assembly of lipid rafts (Simons and Ikonen 1997). However, Ostermeyer et al. (1999) have shown that GSLs are unnecessary for the formation of detergent-insoluble membrane domains and proposed that detergent-insoluble L_o domains are formed by phospholipids containing long saturated fatty acyl chains and cholesterol. Subsequently, Wang et al. (2000) have reported that monounsaturated and shorter chain saturated phospholipids also partition into the L_o phase. Our data confirm that cholesterol is the key component responsible for the formation of L_o domains in the membrane. Undisputedly, GSLs are enriched in the detergent-insoluble membrane fractions and these fractions elicit the characteristics of the L_o domains. The precise reasons for this partitioning of GSLs into the lipid rafts are yet to be established. We observed that GSLs bring about heterogeneity in the membranes and a considerable heterogeneity exists among the L_o domains in the DRM (as revealed by large F_w values). It is likely that specific GSLs segregate into separate microdomains, giving rise to functionally distinct lipid rafts. Recently, Schnaar and co-workers (Vyas et al. 2001) probed the distribution of gangliosides GM1 and GD3 in artificial supported monolayers and neuronal membranes using immunocytochemical labelling and fluorescence resonance energy transfer. They found that GM1 does not co-localize with GD3 and the membrane raft resident proteins Lyn and caveolin both co-localize with GD3.

In conclusion, our data demonstrate that in the presence of high cholesterol concentrations the bulk of the PM can exist in the L_o phase. Although cholesterol is the key component responsible for the formation of L_o domains, membrane proteins and GSLs play a significant role in the organization of these microdomains. Furthermore, it reveals that lipid rafts are heterogeneous. Such heterogeneity may have implications in the functional fine-tuning of lipid rafts.

Acknowledgements This work was supported by the Council of Scientific and Industrial Research, New Delhi, India.

References

Ahmed SN, Brown DA, London E (1997) On the origin of sphingolipid/cholesterol rich detergent-insoluble cell membranes: physiological concentrations of cholesterol and sphingolipid induce formation of a detergent-insoluble, liquid-ordered lipid phase in model membranes. Biochemistry 36:10944–10953

Almeida PF, Vaz WLC, Thompson TE (1992) Lateral diffusion and percolation in two-phase, two component lipid bilayers. Topology of the solid phase domains in-plane and across the lipid bilayers. Biochemistry 31:6739–6747

Amundson DM, Zhou M (1999) Fluorometric method for the enzymatic determination of cholesterol. J Biochem Biophys Methods 38:43–52

Barrow DA, Lentz BR (1985) Membrane structural domains. Resolution limits using diphenylhexatriene fluorescence decay. Biophys J 48:221–234

Bartlett GR (1959) Phosphorous assay in column chromatography. J Biol Chem 234:466–468

Beecham JM, Gratton E, Ameloot M, Knutson JR, Brand L (1991) In: Lackowicz JR (ed) Topics in fluorescence spectroscopy, Plenum Press, New York, pp 241–301

Bernsdorff CA, Wolf A, Winter R, Gratton E (1997) Effect of hydrostatic pressure on water penetration and rotational dynamics in phospholipid-cholesterol bilayers. Biophys J 72:1264–1277

Brown DA, London E (1997) Structure of detergent-resistant membrane domains: does phase separation occur in biological membranes? Biochem Biophys Res Commun 240:1–7

Brown DA, London E (1998) Structure and origin of ordered lipid domains in biological membranes. J Membr Biol 164:103–114

Brown DA and Rose JK (1992) Sorting of GPI-anchored proteins to glycolipid-enriched membrane subdomains during transport to the apical cell surface. Cell 68:533–544

Bunow MR, Bunow B (1979) Phase behavior of ganglioside-lecithin mixtures, relation to dispersion of gangliosides in membranes. Biophys J 27:325–337

Derry DM, Wolfe LS (1967) Gangliosides in isolated neurons and glial cells. Science 158:1450–1452

Dietrich C, Volovyk ZN, Levi M, Thompson NL, Jacobson K (2001) Partitioning of Thy-1, GM1 and cross-linked phospholipid analogs into lipid rafts reconstituted in supported model membrane monolayers. Proc Natl Acad Sci USA 98:10642–10647

Folch J, Lees M, Sloane-Stanley GH (1957) A simple method for the isolation and purification of total lipids from animal tissues. J Biol Chem 226:497–509

Fra AM, Williamson E, Simons K, Parton RG (1994) Detergent-insoluble glycolipid microdomains in lymphocytes in the absence of caveolae. J Biol Chem 269:30745–30748

Friedrichson T, Kurzchalia TV (1998) Microdomains of GPI-anchored proteins in living cells revealed by crosslinking. Nature 394:802–805

Ge M, Field KA, Aneja R, Holowka D, Baird B, Freed JH (1999) Electron spin resonance characterization of liquid ordered phase of detergent-resistant membranes from RBL-2H3 cells. Biophys J 77:925–933

Gidwani A, Holowka D, Baird B (2001) Fluorescence anisotropy measurements of lipid order in plasma membranes and lipid rafts from RBL-2H3 mast cells. Biochemistry 40:12422–12429

Gorodinsky A, Harris DA (1995) Glycolipid-anchored proteins in neuroblastoma cells form detergent-resistant complexes without caveolin. J Cell Biol 129:619–627

Guerold B, Massarelli R, Forster V, Frevsz L, Dreyfus H (1992) Exogenous gangliosides modulate calcium fluxes in cultured neuronal cells. J Neurosci Res 32:110–115

Harder T, Simons K (1997) Caveolae, DIGs and the dynamics of sphingolipid-cholesterol microdomains. Curr Opin Cell Biol 9:534–542

Hinz HJ, Korner O, Nicolau C (1981) Influence of ganglioside GM1 and GD1a on structural and thermotropic properties of small 1,2-dipalmitoyl L-α phosphatidylcholine vesicles. Biochim Biophys Acta 643:557–571

Huang TH, Lee CW, Das Gupta SK, Blume A, Griffin RG (1993) A ^{13}C and ^{2}H nuclear magnetic resonance study of phosphatidylcholine/cholesterol interactions: characterization of liquid-gel phases. Biochemistry 32:13277–13287

Huang Z, Haughland RP (1991) Partition coefficients of fluorescent probes with phospholipid membranes. Biochem Biophys Res Commun 181:166–171

Ipsen JH, Karlstrom G, Mouritsen OG, Wennerstrom HW, Zuckermann MJ (1987) Phase equilibria in the phosphatidylcholine-cholesterol system. Biochim Biophys Acta 905:162–172

Joshi PG, Mishra S (1992) Galactocerebroside mediates Ca^{2+} signaling in cultured glioma cells. Brain Res 597:108–113

Kasahara K, Sanai Y (1999) Possible roles of glycosphingolipids in lipid rafts. Biophys Chem 82:121–127

Korlach J, Schwille P, Webb WW, Feigensen GW (1999) Characterization of lipid bilayer phases by confocal microscopy and fluorescence correlation spectroscopy. Proc Natl Acad Sci USA 96:8461–8466

Kurzchalia TV, Parton RG (1999). Membrane microdomains and caveolae. Curr Opin Cell Biol 11:424–431

Lentz BR, Barenholz Y, Thompson TE (1976). Fluorescence depolarization studies of phase transitions and fluidity in phospholipid bilayers. 2. Two-component phosphatidyl-choline liposomes. Biochemistry 15:4529–4537

Lentz BR, Barrow DA, Hoechli M (1980) Cholesterol-phosphatidylcholine interactions in multilamellar vesicles. Biochemistry 19:1943–1954

Mateo CR, Acuna U, Brochon JC (1995) Liquid-crystalline phases of cholesterol/lipid bilayers as revealed by the fluorescence of *trans*-parinaric acid. Biophys J 68:121–127

Mitchell DC, Litman BJ (1998) Effect of cholesterol on molecular order and dynamics in highly polyunsaturated phospholipid bilayers. Biophys J 75:896–908

Ostermeyer AG, Beckrich BT, Ivarson KA, Grove KE, Brown DA (1999) Glycosphingolipids are not essential for formation of detergent-resistant membrane rafts in melanoma cells. Methyl-beta-cyclodextrin does not affect cell surface transport of a GPI-anchored protein. J Biol Chem 274:34459–34466

Prendergast FG, Haugland RP, Callahan PJ (1981) 1-[4-(Trimethylamino)phenyl]-6-phenylhexa-1,3,5-triene: synthesis, fluorescence properties, and use as a fluorescence probe of lipid bilayers. Biochemistry 20:7333–7338

Ravichandra B, Joshi PG (1999) Gangliosides asymmetrically alter the membrane order in cultured PC-12 cells. Biophys Chem 76:117–132

Rawat SS, Mukherjee S, Chattopadhyay A (1997) Micellar organization and dynamics: a wavelength selective fluorescence approach. J Phys Chem 101:1922–1929

Rietveld A, Simons K (1998) The differential miscibility of lipids as the basis for the formation of functional membrane rafts. Biochim Biophys Acta 1376:467–479

Rodgers W, Crise B, Rose JK (1994) Signals determining protein tyrosine kinase and glycosyl-phosphatidylinositol-anchored protein targeting to a glycolipid-enriched membrane fraction. Mol Cell Biol 14:5384–5391

Sanganahalli BG, Joshi PG, Joshi NB (2000) Differential effects of tricyclic anti-depressant drugs on membrane dynamics: a fluorescence spectroscopic study. Life Sci 6:81–90

Sankaram MB, Thompson TE (1991) Cholesterol-induced fluid-phase immiscibility in membranes. Proc Natl Acad Sci USA 88:8686–8690

Schroeder R, London E, Brown D (1994) Interactions between saturated acyl chains confer detergent resistance on lipids and glycosylphosphatidylinositol (GPI)-anchored proteins: GPI-anchored proteins in liposomes and cells show similar behavior. Proc Natl Acad Sci USA 91:12130–12134

Sharma M, Joshi PG, Joshi NB (1997) Alterations in plasma membrane of glioblastoma cells by photodynamic action of merocyanine 540. Biochim Biophys Acta 1323:272–280

Shinitzky M, Barenholz Y (1978) Fluidity parameters of lipid regions determined by fluorescence polarization. Biochim Biophys Acta 515:367–395

Sillerud LO, Schafer DE, Yu RK, Konigsberg WH (1979) Calorimetric properties of mixtures of ganglioside GM1 and dipalmitoylphosphatidylcholine. J Biol Chem 254:10876–10880

Simons K, Ikonen E (1997) Functional rafts in cell membranes. Nature 387:569–572

Simons K, Toomre D (2000) Lipid rafts and signal transduction. Nat Rev Mol Cell Biol 1:31–39

Sreenivasan R, Joshi PG, Joshi NB (1997) Structural perturbations induced by photodynamic action of porphyrin aggregates on plasma membrane and microsomes of glioblastoma cells. J Photosci 4:41–48

Straume M, Litman BJ (1987) Influence of cholesterol on equilibrium and dynamic bilayer structure of unsaturated acyl chain phosphatidylcholine vesicles as determined from higher order analysis of fluorescence anisotropy decay. Biochemistry 26:5121–5126

Varma R, Mayor S (1998) GPI-anchored proteins are organized in submicron domains at the cell surface. Nature 394:798–801

Vist MR, Davis JH (1990) Phase equilibria of cholesterol/dipalmitoylphosphatidylcholine mixtures: ^{2}H nuclear magnetic resonance and differential scanning calorimetry. Biochemistry 29:451–464

Vyas KA, Patel HV, Vyas AA, Schnaar RL (2001) Segregation of gangliosides GM1 and GD3 on cell membranes, isolated membrane rafts, and defined supported lipid monolayers. Biol Chem 382:241–250

Wang TY, Leventis R, Silvius JR (2000) Fluorescence-based evaluation of the partitioning of lipids and lipidated peptides into liquid-ordered lipid microdomains: a model for molecular partitioning into ''lipid rafts''. Biophys J 79:919–933

Williams BW, Stubbs CD (1988) Properties influencing fluorophore lifetime distributions in lipid bilayers. Biochemistry 27:7994–7999

Xiang TH, Anderson BD (1998) Phase structures of binary lipid bilayers as revealed by permeability of small molecules. Biochim Biophys Acta 1370:64–76